



Article

Syntheses, Structures, and Catalytic Hydrocarbon Oxidation Properties of *N*-Heterocycle-Sulfonated Schiff Base Copper(II) Complexes

Susanta Hazra *, Bruno G. M. Rocha, M. Fátima C. Guedes da Silva *, Anirban Karmakar and Armando J. L. Pombeiro *

Centro de Química Estrutural, Instituto Superior Técnico, Universidade de Lisboa, Av. Rovisco Pais, 1049-001 Lisbon, Portugal; bruno.g.m.rocha@tecnico.ulisboa.pt (B.G.M.R.); anirbanchem@gmail.com (A.K.)

* Correspondence: h.susanta@gmail.com (S.H.); fatima.guedes@tecnico.ulisboa.pt (M.F.C.G.d.S.); pombeiro@tecnico.ulisboa.pt (A.J.L.P.); Tel.: +351-218419260 (S.H. & M.F.C.G.d.S. & A.J.L.P.)

Received: 16 October 2018; Accepted: 31 January 2019; Published: 6 February 2019



Abstract: Reaction of the *o*-[(*o*-hydroxyphenyl)methylideneamino]benzenesulfonic acid (H_2L) (**1**) with $CuCl_2 \cdot 2H_2O$ in the presence of pyridine (py) leads to $[Cu(L)(py)(EtOH)]$ (**2**) which, upon further reaction with 2,2'-bipyridine (bipy), pyrazine (pyr), or piperazine (pip), forms $[Cu(L)(bipy) \cdot MeOH]$ (**3**), $[Cu_2(L)_2(\mu-pyr)(MeOH)_2]$ (**4**), or $[Cu_2(L)_2(\mu-pip)(MeOH)_2]$ (**5**), respectively. The Schiff base (**1**) and the metal complexes (**2–5**) are stabilized by a number of non-covalent interactions to form interesting H-bonded multidimensional polymeric networks (except **3**), such as zigzag 1D chain (in **1**), linear 1D chain (in **2**), hacksaw double chain 1D (in **4**) and 2D motifs (in **5**). These copper(II) complexes (**2–5**) catalyze the peroxidative oxidation of cyclic hydrocarbons (cyclooctane, cyclohexane, and cyclohexene) to the corresponding products (alcohol and ketone from alkane; alcohols, ketone, and epoxide from alkene), under mild conditions. For the oxidation of cyclooctane with hydrogen peroxide as oxidant, used as a model reaction, the best yields were generally achieved for complex **3** in the absence of any promoter (20%) or in the presence of py or HNO_3 (26% or 30%, respectively), whereas **2** displayed the highest catalytic activity in the presence of HNO_3 (35%). While the catalytic reactions were significantly faster with py, the best product yields were achieved with the acidic additive.

Keywords: sulfonated Schiff base; copper(II) compounds; pyridine; 2,2'-bipyridine; pyrazine; piperazine; hydrocarbon oxidation

1. Introduction

Over the past decades, there has been a marked development in the coordination chemistry of Schiff base metal complexes [1–29], encouraged by the variety of their solid-state structures [1–3], as well as magnetic [4–9], fluorescence [10–12], and catalytic [1,13–15] properties. Though a large number of Schiff bases of various types, including those containing the carboxylic acid group, has been reported [1–18], sulfonic acid containing Schiff bases are rare and only a few metal complexes have been investigated [19–29]. Moreover, intra- and intermolecular interactions via sulfonate oxygens could generate interesting multinuclear copper complexes [19,20,22,28] which may be useful for further catalytic application.

In fact, sulfonated Schiff bases display versatile complex formation abilities leading, for example, to mono-, di-, or polymeric structures [19–29]. In an earlier study, we reported that the Schiff base 2-[(2-hydroxyphenyl)methylideneamino]benzenesulfonic acid (H_2L) can form solvatomorphs which have identical basic structures but with different non-coordinated solvents [22].

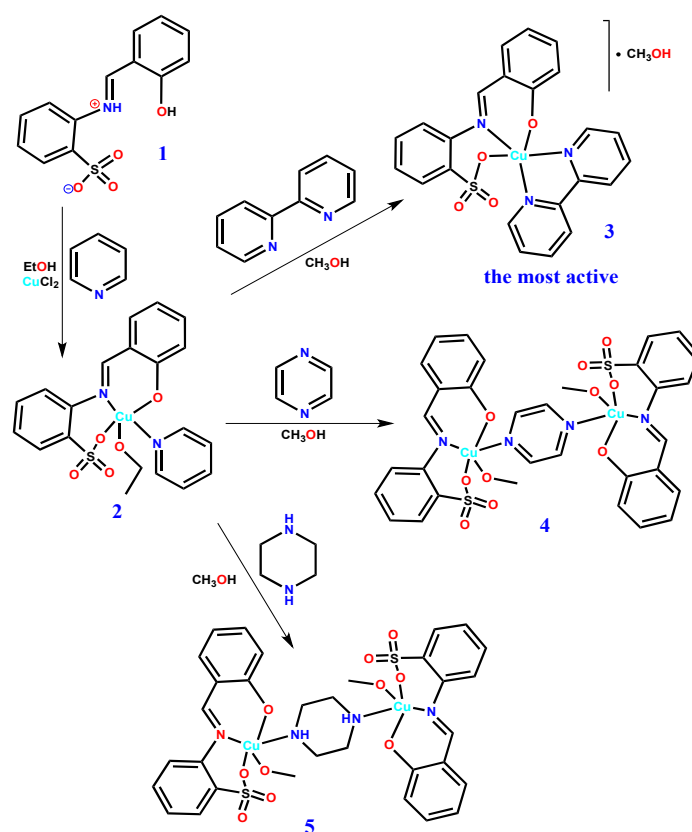
We also obtained a bis(μ_4 -(*ae*)-cyclohexane-1,4-dicarboxylato-O,O',O'',O''')-tetracopper [19,23], two carboxylate-sulfonated copper polymers [28], and three pseudohalide-bridged copper complexes [20] containing 2-(2-pyridylmethyleneamino)benzenesulfonate. The tetranuclear [19,23] and polymeric copper complexes were efficient catalysts [28] for the cyclohexane oxidation in both conventional ($\text{CH}_3\text{CN}/\text{H}_2\text{O}$) [19,28] and non-conventional (ionic liquid) solvents [23,28], whereas the pseudohalide complexes [20] were found to catalyze the Henry reaction in aqueous medium. Recently, we reported another new sulfonated Schiff base, 2-[(2-hydroxy-3-methoxyphenyl)methylideneamino]benzenesulfonic acid, which was utilized to synthesize a few mono- and dicopper complexes [24,27]. Interestingly, the dimeric complexes were found to be highly efficient catalysts for the microwave-assisted oxidation of 1-phenylethanol under mild conditions and in the absence of any additive [24].

The curious molecular structures and catalytic properties of such compounds [19–29] inspired us (i) to synthesize other copper complexes of the sulfonated Schiff base ligand L^{2-} and (ii) to apply them in alkane oxidation studies.

Saturated hydrocarbons are rarely used as starting materials in the chemical industry due to their low reactivity, despite being the most abundant and least expensive potential carbon sources for the organic synthesis of functionalized valuable products [30–43]. Peroxidative oxidation [30–67] of alkanes is a promising approach for the synthesis of the corresponding alcohols and ketones. In particular, oxidation with environmentally friendly oxidants, such as hydrogen peroxide (H_2O_2) [30–67] or dioxygen [68–71], is a topic of great interest, and the use of copper complexes as catalysts [19,28,44,45,47,48] is particularly promising. However, the catalytic efficiency has still to be improved, which accounts for another aim of the current study.

Moreover, in view of the multi-copper nature of particulate methane monooxygenase (pMMO), an enzyme that catalyzes the oxidation of alkanes to alcohols, particular attention [47–50,72–75] should be paid to multinuclear copper catalysts, a topic which also concerns this work.

Hence, due to the above considerations, and also inspired by our previous successful catalytic application of a tetracopper(II) complex containing a mixed ligand (carboxylate and sulfonate) in the peroxidative oxidation of cyclohexane [19] and by the fact that *N*-heterocyclic bases can promote the reaction [30–67], we anticipated that copper(II) complexes bearing a mixed ligand system of sulfonate and a *N*-heterocyclic base could be also particularly active for alkane oxidation. Thus, in the present study, we investigate the reactions of the sulfonated Schiff base 2-[(2-hydroxyphenyl)methylideneamino]benzenesulfonic acid (H_2L , **1**) [21,22] with $\text{CuCl}_2 \cdot 2\text{H}_2\text{O}$ and a *N*-heterocyclic base, such as pyridine (py), 2,2'-bipyridine (bipy), pyrazine (pyr), or piperazine (pip) (Scheme 1). Herein, we report the syntheses, structures, and hydrocarbon oxidation properties of the two new mononuclear complexes $[\text{Cu}(\text{L})(\text{py})(\text{EtOH})]$ (**2**) and $[\text{Cu}(\text{L})(\text{bipy})] \cdot \text{MeOH}$ (**3**) and the two new dinuclear compounds $[\text{Cu}_2(\text{L})_2(\mu\text{-pyr})(\text{MeOH})_2]$ (**4**) and $[\text{Cu}_2(\text{L})_2(\mu\text{-pip})(\text{MeOH})_2]$ (**5**) with such ligands.



Scheme 1. Syntheses of 2–5 from 1.

2. Results and Discussion

2.1. Syntheses and Characterization

The [1+1] condensation of salicylaldehyde and 2-aminobenzenesulfonic acid in aqueous methanol (1:2) leads to the formation of the Schiff base H_2L (1) [21,22] which, upon reaction with $\text{CuCl}_2 \cdot 2\text{H}_2\text{O}$ in ethanol and in the presence of pyridine (py), produces the mononuclear copper(II) complex $[\text{Cu}(\text{L})(\text{py})(\text{EtOH})]$ (2) (Scheme 1). Furthermore, the replacement of the pyridine moiety of 2 with 2,2'-bipyridine (bipy), pyrazine (pyr), and piperazine (pip) in methanol produces the corresponding complexes $[\text{Cu}(\text{L})(\text{bipy})] \cdot \text{MeOH}$ (3), $[\text{Cu}_2(\text{L})_2(\mu\text{-pyr})(\text{MeOH})_2]$ (4), and $[\text{Cu}_2(\text{L})_2(\mu\text{-pip})(\text{MeOH})_2]$ (5), which were characterized by elemental microanalysis, IR spectroscopy, and single crystal X-ray diffraction study. The Schiff base H_2L (1) was characterized by both NMR and single crystal X-ray diffraction analyses. All the compounds including the Schiff base were isolated in very good yields (92–78%).

The IR spectrum of the Schiff base H_2L (1) exhibits the expected bands at 1638 cm^{-1} and 1376 cm^{-1} , which are indicative of the $\text{C}=\text{N}$ bond and the sulfonate group, respectively. In the IR spectra of the metal complexes (2–5), the $\nu(\text{C}=\text{N})$ bands are observed in the range of $1606\text{--}1613 \text{ cm}^{-1}$, whereas the sulfonate groups are evidenced by the medium intense bands at the $1382\text{--}1386 \text{ cm}^{-1}$ range.

2.2. Description of Crystal Structures of 1–5

2.2.1. Crystal Structure of H_2L (1)

The asymmetric unit of H_2L (1) (Figure 1) contains two symmetry-independent molecules of the Schiff base with relative positions slightly shifted from perpendicular as evidenced by the angle of 80.46° between the least-square planes of the two units. The two molecules superimpose quite well only with a slight discrepancy in the angle between the least-square planes of the aromatic rings,

which assume values of 8.41° for one molecule and 10.98° for the other (Table 1). The azomethine linkages in **1** are evident from the N–C bond lengths (1.299(4) and 1.294(4) Å (Table 1). The molecules are stabilized by intramolecular hydrogen bonds involving the imino nitrogen atoms (as donors) and both the phenolic and sulfonate oxygen atoms (as acceptors) (Figure 1; Table S1, Supplementary Materials). The crystal structure is stabilized by intermolecular H-contacts involving the phenolic oxygen atoms (as donor) of one molecule and the sulfonate oxygen atoms (as acceptor) of another molecule (Figure 1).

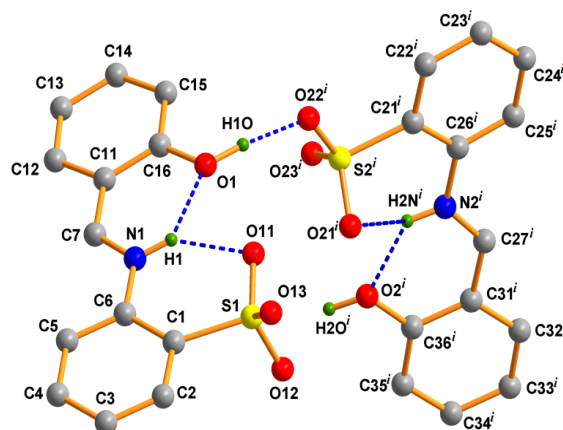


Figure 1. Ball and stick presentation of the crystal structure of **1**. All H-atoms except those participating in H-bonding are omitted for clarity. Symmetry: $-x, 1-y, -z$.

Table 1. Comparison of some selected features of Schiff base **1** and complexes **2–5**. Distances in (Å) and angles in ($^\circ$).

	1	2	3	4	5
<i>In the Organic Moiety H₂L (or L²⁻)</i>					
C–N _{imino}	1.299(4) 1.294(4)	1.303(4)	1.292(3)	1.301(3)	1.309(5)
C _{aromatic} –N _{imino}	1.433(4) 1.438(4)	1.429(4)	1.434(3)	1.426(3)	1.429(5)
Coplanarity of aromatic rings ($^\circ$)	8.41 10.98	58.19	62.01	51.04	51.81
<i>Surrounding the Copper Atom</i>					
Cu–N _{imino}	-	1.976(2)	1.9837(19)	1.9769(17)	1.975(3)
Cu–O _{sulfonato}	-	2.014(2)	2.3789(18)	1.9733(16)	2.019(3)
Cu–O _{phenoxido}	-	1.898(2)	1.8942(18)	1.8770(16)	1.900(3)
Cu–N _{coligand}	-	2.015(3)	2.009(2) 2.061(2)	2.0709(17)	2.004(3)
Cu–O _{coligand}	-	2.290(2)	-	2.3760(18)	2.303(3)
\angle N–Cu–N	-	177.98(10)	79.71(8) 102.71(8) 170.85(8)	174.06(7)	177.57(14)
\angle O _{sulfonato} –Cu– O _{phenoxido}	-	157.30(9)	113.95(8)	158.97(8)	151.07(14)
Cu coordination environment	-	N ₂ O ₃	N ₃ O ₂	N ₂ O ₃	N ₂ O ₃
τ_5	-	0.35	0.27	0.25	0.44
Cu \cdots Cu (minimum)	-	7.541	8.110	6.919	6.782

2.2.2. Crystal Structures of 2–5

The crystal structures of $[\text{Cu}(\text{L})(\text{py})(\text{EtOH})]$ (**2**), $[\text{Cu}(\text{L})(\text{bipy})]\cdot\text{MeOH}$ (**3**), $[\text{Cu}_2(\text{L})_2(\mu\text{-pyr})(\text{MeOH})_2]$ (**4**), and $[\text{Cu}_2(\text{L})_2(\mu\text{-pip})(\text{MeOH})_2]$ (**5**) are shown in Figure 2. The single crystal X-ray diffraction analyses show that **2** and **3** are mononuclear copper(II) complexes, whereas **4** and **5** are dicopper(II) compounds bridged by pyrazine and piperazine, respectively. In all cases, the metal center adopts distorted square pyramid geometries (τ_5 parameter in the 0.25–0.44 range, Table 1) and the L^{2-} ligand acts as an $\text{O},\text{N},\text{O}$ -chelator by means of the phenolic O-, the imine N-, and one sulfonate O-atoms. The coordination sphere of copper is then fulfilled either by another chelating molecule (**3**) leading to a N_3O_2 metal environment, or by a solvent and one more organic moiety (**2**, **4**, and **5**) and forming N_2O_3 settings (Table 1). Probably as a result of the chelating mode of bipyridine, compound **3** is the only one in which the L^{2-} ligand occupies both equatorial ($\text{O}_{\text{phenoxido}}$ and N_{imino} atoms) and apical ($\text{O}_{\text{sulfonato}}$) sites, thus contrasting with the other complexes (**2**, **4**, and **5**) in which it occupies three of the equatorial positions.

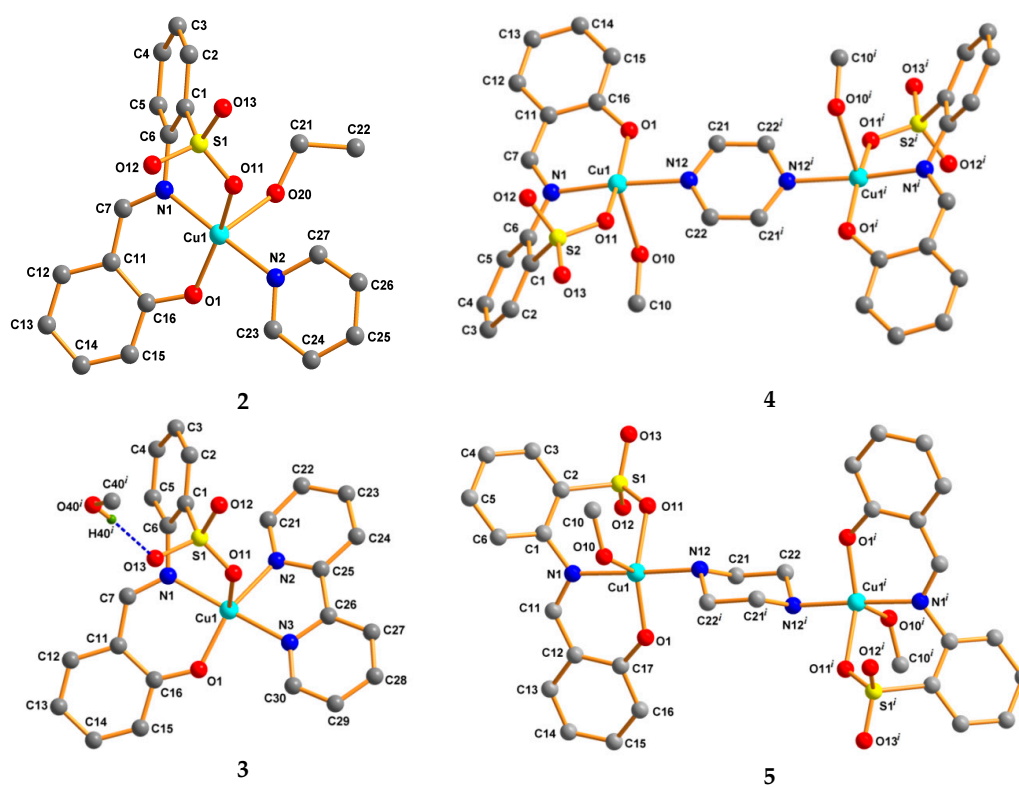


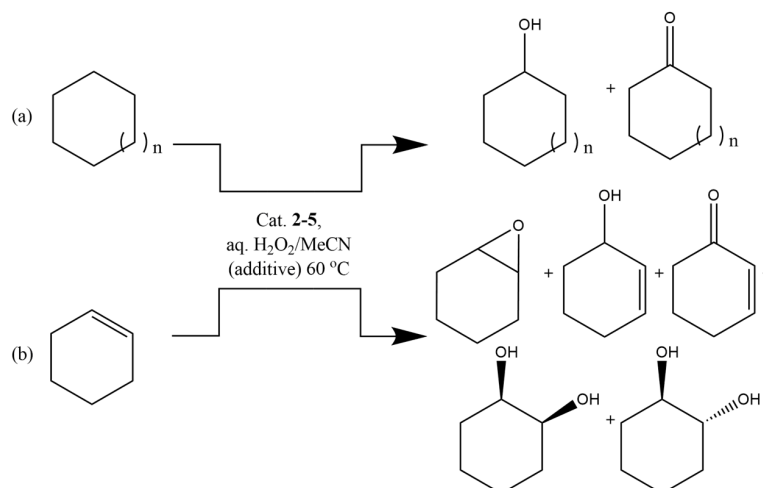
Figure 2. Idealized ball and stick presentation of the crystal structures of **2–5**. All H-atoms except those participating in H-bonding are omitted for clarity. Symmetry: $x, y, -1+z$ (in **3**), $1-x, -y, 1-z$ (in **4**), and $2-x, -y, -z$ (in **5**).

The $\text{Cu}-\text{N}_{\text{imino}}$ bond distances in the structures of all complexes lie in the 1.975(3)–1.9837(19) Å range (Table 1) and are slightly shorter than those involving the metal and the other N-ligands (2.004(3)–2.0709(17) Å). Concerning the copper–oxygen lengths, the $\text{Cu}-\text{O}_{\text{phenoxido}}$ distances (1.8770(16)–1.900(3) Å) are considerably shorter than the $\text{Cu}-\text{O}_{\text{sulfonato}}$ ones whose minimum value is 1.9733(16) Å. In this respect, the longest value of 2.3789(18) Å found for **3** relates with the metal–oxygen distances for the axial sites (i.e., $\text{Cu}-\text{O}_{\text{coligand}}$ lengths, Table 1) and is due to the Jahn–Teller effect.

2.2.3. Oxidation of Hydrocarbons

The catalytic properties of the copper(II) complexes (**2–5**) in the peroxidative oxidation of hydrocarbons (cyclooctane, cyclohexane, and cyclohexene) to the corresponding alcohols, ketone,

and epoxide, under mild conditions, were evaluated. Inspired by our previous findings [19,53], we chose as a model system the reaction of peroxidative oxidation of cyclooctane using hydrogen peroxide as oxidant. The catalytic procedure ran at 60 °C in acetonitrile and the reactions were monitored by GC with a typical catalyst loading (per copper) of approximately 1×10^{-3} M (Scheme 2).



Scheme 2. Peroxidative oxidation of hydrocarbons [(a) cyclohexane ($n = 1$) or cyclooctane ($n = 3$) and (b) cyclohexene] to the corresponding products, with aqueous H₂O₂, catalyzed by the copper(II) complexes 2–5, in the presence or absence of any additive, under typical mild reaction conditions of this work.

Among all the catalysts studied in this reaction, the mononuclear complex **3** was the most effective one. In fact, after 1 h of reaction time and in the absence of any additive, it led to an overall turnover number (TON) up to 50 moles of products per mole of catalyst (Table 2, entry 11) and an overall yield of approximately 20% based on cyclooctane. Compound **5** exhibited a lower activity, followed by compounds **2** and **4** that were the least active ones under these conditions (Table 3, entry 15; Table 4, entry 14; Table 5, entry 14; respectively). The yield accumulation of the oxygenates (cyclooctanol and cyclooctanone) over the reaction time of 2–5 in the model system is shown in Figure 3.

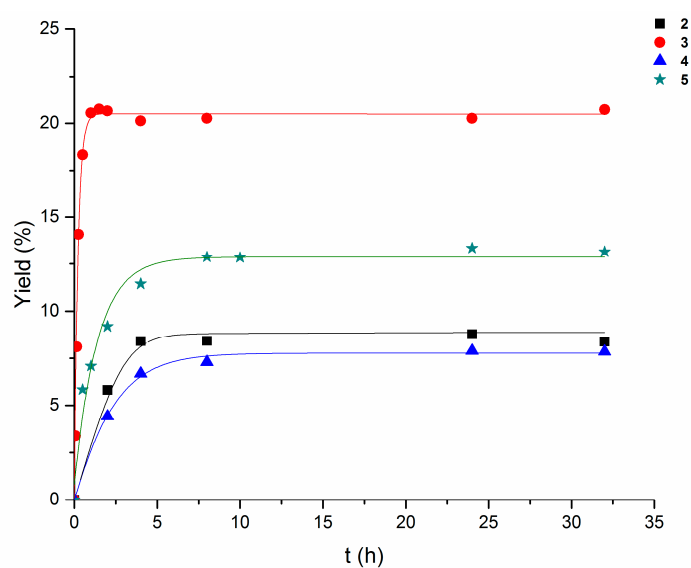


Figure 3. Accumulation of oxygenates with time in the cyclooctane (initial concentration 0.25 M) oxidation with H₂O₂ (1.2 M) catalyzed by 2–5 in acetonitrile at 60 °C.

Table 2. Effect of the presence of an additive in the oxidation of cyclooctane catalyzed by **3** ^a.

Entry	Time (min)	No Additive			py			HNO ₃		
		Yield ^b (%)	Selectivity ^c	TON ^d	Yield ^b (%)	Selectivity ^c	TON ^d	Yield ^b (%)	Selectivity ^c	TON ^d
1	0	0	-	0	0	-	0	0	-	0
2	1				3	0:100	8			
3	3				9	1:99	23			
4	4	3	1:99	8	14	4:96	35	13	1:99	31
5	5.5				23	7:93	58			
6	7				26	11:89	65			
7	9	8	3:97	20	26	14:86	65			
8	10				26	21:79	65	14	2:98	35
9	15	14	5:95	35	26	24:76	65			
10	30	18	6:94	45	26	28:72	65	17	3:97	42
11	60	20	10:90	50	26	27:73	65			
12	90	20	17:83	50	26	29:71	65	19	5:95	47
13	2 × 60	20	20:80	50	26	34:66	65	20	7:93	50
14	4 × 60	20	23:77	50	26	37:63	65	22	10:90	56
15	5.5 × 60							23	10:90	58
16	8 × 60	20	27:73	51	26	39:61	65	25	11:89	63
17	10 × 60							27	11:89	68
18	16 × 60							30	13:87	74
19	21.5 × 60							26	20:80	65
20	24 × 60	20	31:69	50	26	53:47	65	25	20:80	62
21	29.5 × 60							20	23:77	50
22	32 × 60	20	36:64	51	26	54:46	65	18	25:75	46

^a Reaction conditions: cyclooctane (0.25 M), complex **3** (10^{-3} M), additive (0.072 M), H₂O₂ (1.2 M) in acetonitrile at 60 °C; total volume of reaction mixture is 10 mL. ^b Amounts of cyclooctanone and cyclooctanol were determined after reduction of the aliquots with solid PPh₃ (for this method, see references [61–65]). ^c Cyclooctanone/cyclooctanol ratio. ^d Turnover number of the catalyst (sum of moles of all products per mole of **3**).

Blank experiments confirmed that no cyclooctanol or cyclooctanone are formed appreciably in the absence of the complexes (**2–5**). The Schiff base H₂L (**1**) is inactive (Table S2, Supplementary Materials) toward the cyclooctane oxidation, whereas CuCl₂ produces insignificant amounts of products, that is, <3% of total yield can be detected.

The peroxidative oxidation of hydrocarbons catalyzed, for example, by some copper complexes can proceed more efficiently in the presence of a suitable additive [53], and thus we tested pyridine (py) and HNO₃ as a basic and an acid promoter, respectively.

For all the complexes **2–5**, the presence of such additives resulted, in general, in an enhancement of the maximum yield and TON values, mainly in the case of HNO₃ (Tables 2–5). Changes in selectivity were also observed.

All the catalysts **2–5** exhibit comparable overall yields (Tables 2–5) in the presence of pyridine after a sufficiently long reaction time (e.g., 24 h). However, the differences in reaction rates are clearly observed in the first 15 min-period (Figure 4).

Table 3. Effect of the presence of an additive in the oxidation of cyclooctane catalyzed by 5^a.

Entry	Time(min)	No Additive			py			HNO ₃		
		Yield _b (%)	Selectivity _c	TON ^d	Yield _b (%)	Selectivity _c	TON ^d	Yield _b (%)	Selectivity _c	TON ^d
1	0	0	-	0	0	-	0	0	-	0
2	1				1	0:100	3			
3	3				5	3:97	13			
4	4				7	4:96	17			
5	6				13	5:95	33			
6	8				18	7:93	45			
7	10				23	8:92	58			
8	15				23	16:84	58	3	0:100	8
9	30	6	2:98	15	23	21:79	58	6	0:100	15
10	60	7	3:97	18	23	26:74	58	8	1:98	19
11	90				23	27:73	58	10	1:98	25
12	2 × 60	9	3:97	23	23	29:71	58	12	2:98	31
13	3 × 60							19		47
14	4 × 60	11	9:91	28	23	34:66	58	30	3:97	76
15	8 × 60	13	23:77	32	23	40:60	58	26	23:77	64
16	10 × 60	13	28:72	31						
17	24 × 60	13	34:66	32	23	56:44	58	15	34:66	37
18	32 × 60	13	39:61	31	23	61:39	58	13	39:61	32

^a Reaction conditions: cyclooctane (0.25 M), complex 5 (10⁻³ M per copper), additive (0.072 M), H₂O₂ (1.2 M) in acetonitrile at 60 °C; total volume of reaction mixture is 10 mL. ^b Amounts of cyclooctanone and cyclooctanol were determined after reduction of the aliquots with solid PPh₃ (for this method, see references [61–65]). ^c Cyclooctanone/cyclooctanol ratio. ^d Turnover number of the catalyst (sum of moles of all products per mole of 5).

Table 4. Effect of the presence of an additive in the oxidation of cyclooctane catalyzed by 2^a.

Entry	Time(h)	No Additive			py			HNO ₃		
		Yield _b (%)	Selectivity _c	TON ^d	Yield _b (%)	Selectivity _c	TON ^d	Yield _b (%)	Selectivity _c	TON ^d
1	0	0	-	0	0	-	0	0	-	0
2	1				3	0:100	8			
3	3				9	3:97	23			
4	4				15	12:88	38			
5	5.5				19	20:80	48			
6	7				21	22:78	53			
7	9				23	25:75	58			
8	10				24	26:74	60			
9	15				24	27:73	60	3	0:100	7.5
10	30				24	29:71	60	8	0:100	20
11	60				24	30:70	60	16	0:100	40
12	90							22	1:98	55
13	2 × 60	6	0:100	16	24	32:68	60	31	2:98	78
14	4 × 60	8	2:98	20	24	34:66	60	35	2:98	88
15	8 × 60	8	4:96	21	24	39:61	60	26	5:95	65
16	24 × 60	8	32:68	21	24	49:51	60	20	38:62	50
17	32 × 60	8	36:64	21	24	52:48	60	17	33:67	43

^a Reaction conditions: cyclooctane (0.25 M), complex 2 (10⁻³ M), additive (0.072 M), H₂O₂ (1.2 M) in acetonitrile at 60 °C; total volume of reaction mixture is 10 mL. ^b Amounts of cyclooctanone and cyclooctanol were determined after reduction of the aliquots with solid PPh₃ (for this method, see references [61–65]). ^c Cyclooctanone/cyclooctanol ratio. ^d Turnover number of the catalyst (sum of moles of all products per mole of 2).

Table 5. Effect of the presence of an additive in the oxidation of cyclooctane catalyzed by 4^a.

Entry	Time(min)	No Additive			py			HNO ₃		
		Yield ^b (%)	Selectivity ^c	TON ^d	Yield ^b (%)	Selectivity ^c	TON ^d	Yield ^b (%)	Selectivity ^c	TON ^d
1	0	0	-	0	0	-	0	0	-	0
2	1				1	0:100	3			
3	3				5	0:100	13			
4	4				9	1:99	23			
5	5.5				13	8:92	33			
6	7				17	12:88	43			
7	9				20	15:85	50			
8	10				21	17:83	53			
9	15				23	19:81	58			
10	30				23	26:74	58			
11	60				23	28:72	58	7	0:100	19
12	90				23	30:70	58			
13	2 × 60	4	0:100	11	23	31:69	58	14	2:98	36
14	4 × 60	7	2:98	17	23	36:64	58	27	2:98	68
15	8 × 60	7	3:97	18	23	43:57	58	23	4:96	57
16	10 × 60							24	6:94	59
17	24 × 60	7	26:74	17	23	53:47	58	13	32:68	32
18	32 × 60	7	33:67	18	23	53:47	58	14	37:63	35

^a Reaction conditions: cyclooctane (0.25 M), complex 4 (10^{-3} M per copper), additive (0.072 M), H₂O₂ (1.2 M) in acetonitrile at 60 °C; total volume of reaction mixture is 10 mL. ^b Amounts of cyclooctanone and cyclooctanol were determined after reduction of the aliquots with solid PPh₃ (for this method, see references [61–65]). ^c Cyclooctanone/cyclooctanol ratio. ^d Turnover number of the catalyst (sum of moles of all products per mole of 4).

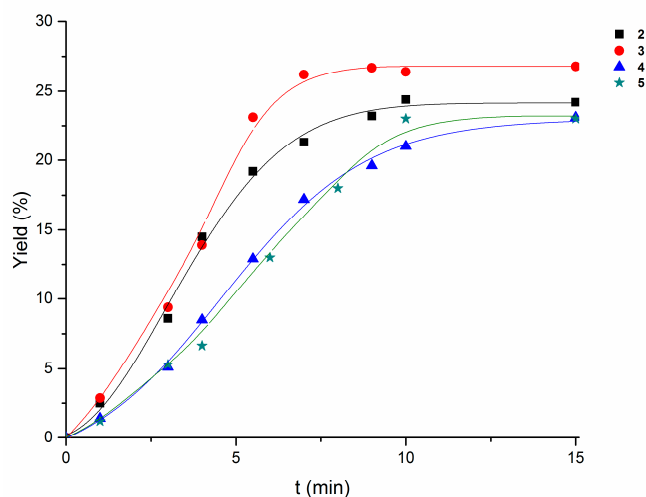


Figure 4. Comparison of the accumulation of oxygenates with time (0–15 min) in the cyclooctane (initial concentration 0.25 M) oxidation with H₂O₂ (1.2 M), in the presence of pyridine (0.072 M), catalyzed by 2–5 (10^{-3} M) in acetonitrile at 60 °C.

In fact, for example, compound 2 in comparison with 4 leads to a higher initial rate of cyclooctane oxidation (Figure 4) and a slightly lower ketone:alcohol selectivity, but a convergence of their behaviors occurs over time in the presence of pyridine, suggesting the eventual conversion of 4 into 2, upon reaction with this base (Tables 4 and 5).

Compound 5 also leads to lower initial rate than 2, but displays a higher selectivity toward the alcohol, comparable to that of 3.

The use of compound **3** (Table 2) results in the highest rate (Figure 4), the highest product yield, and the highest selectivity (comparable to **5**) toward the formation of the alcohol product.

In all the cases, at the maximum product yield, a higher selectivity toward the alcohol is observed, but it decreases over time and eventually reverses. For example, when the maximum yields are accomplished in the reactions with **3** and **5**, the cyclooctanol:cyclooctanone molar ratio is approximately 90:10, but at 24 h of reaction time the inversion of the ketone:alcohol ratio has already occurred (Tables 2 and 3).

The application of HNO_3 as a promoter, instead of pyridine, in the peroxidative oxidation of cyclooctane resulted in a considerable yield promotion (by approximately 10% for reactions using **2** and **5** and by approximately 5% in the case of **3** and **4**) in comparison to the best yields in the reactions in the presence of pyridine. In acidic conditions, the best yield (35%) is obtained with the mononuclear **2** (Figure 5) (curiously, in the presence of pyridine, the best catalyst, **3**, is also mononuclear).

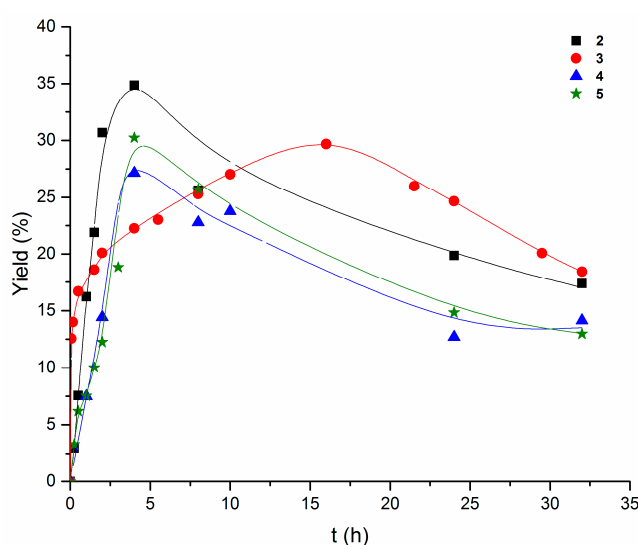


Figure 5. Comparison of the accumulation of oxygenates with time (0–32 h) in the cyclooctane (initial concentration 0.25 M) oxidation with H_2O_2 (1.2 M) in the presence of HNO_3 (0.072 M), catalyzed by **2–5** (10^{-3} M) in acetonitrile at 60 °C.

The drawback of the acidic additive is the slower reactivity when compared to the much faster reactions in the presence of pyridine. In fact, the maximum yield of the cyclooctane oxidation was achieved within a few minutes when pyridine was used as a promoter, whereas when this was replaced by HNO_3 , the reaction time to achieve the maximum yield increased to 4 h, in the cases of compounds **2**, **4**, and **5**, and to 16 h for **3** (Figure 5).

Contrary to what happens in the reactions in the presence of pyridine, those with HNO_3 do not follow a clear pattern (Figure 5).

The cyclooctanol/cyclooctanone ratio in acidic conditions, when the maximum yield is achieved, is better (for **2**, **4**, and **5**) or comparable (in the case of **3**) to that observed when pyridine is used as additive. As in the case of the basic promoter, the highest yield corresponds to a marked alcohol predominance over the ketone (approximately 98:2 ratio for **2**, **4**, and **5**) but over the reaction time this selectivity decreases (as the overall yield does) although without reversing, thus also attesting to the better selectivity toward the alcohol for compounds **2–5** using the HNO_3 promoter.

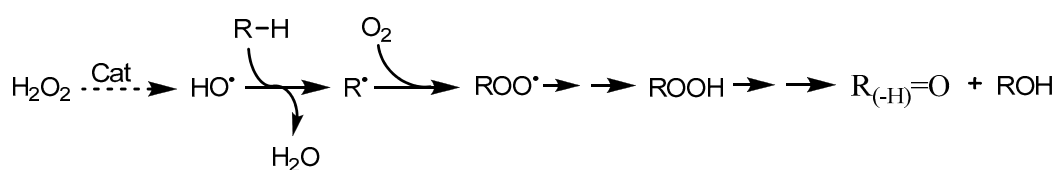
In order to get an insight into the reaction mechanism, we selected the overall best (with and without additives) catalyst, **3**, and studied the effect of the addition of Ph_2NH , an oxygen radical trap [37], and the effect of the addition of CBrCl_3 , a carbon radical trap [37], on the cyclooctane oxidation.

The addition of either Ph₂NH or CBrCl₃, in a stoichiometric amount relative to H₂O₂ or cyclooctane, respectively, leads to approximately 5–8%, 29–32%, and 54% suppression of the products formation for 4, 9, and 120 min reaction time, respectively (Tables S4 and S5, Supplementary Materials, entries 2–4). Thus, the cyclooctane oxidation reaction appears to proceed mainly via a non-free radical pathway for short reaction times, although over time a free radical mechanism becomes more pronounced.

This is also consistent with the high selectivity toward the alcohol at short reaction times, which decreases during the reaction. For shorter reaction times, such a behavior supports the predominance of a non-free radical pathway conceivably associated with a metal-centered oxidant instead of a free HO• radical [58]. Various mechanistic possibilities can be postulated [47,48,57,58].

For the free radical mechanism, a plausible pathway can be suggested [31,32,44,46,57,58] to involve the metal-assisted decomposition of H₂O₂ into the hydroxyl radical HO• which then abstracts H• from RH to give the alkyl radical R•. The formation of HO• from H₂O₂ involves proton-transfer steps among H₂O₂, hydroperoxo-, peroxy-, and oxo-metal species [34,47–50].

As presented in Scheme 3, R• either reacts with molecular oxygen producing ROO• (which upon H-abstraction, for example, from H₂O₂ or the derived H₂O• radical, forms alkylhydroperoxide ROOH) or reacts with a possible metal-hydroperoxo intermediate species [Cu]–OOH producing ROOH. This organoperoxide then undergoes metal-promoted decomposition to form O-centered organo radicals, RO• (upon O–O bond cleavage), and ROO• (upon O–H bond rupture). While the H-abstraction from RH by RO• leads to the formation of ROH, the decomposition of ROO• produces ROH and the corresponding ketone R_(-H)=O.



Scheme 3. Radical mechanism of the peroxidative oxidation of hydrocarbons with H₂O₂.

In agreement with such mechanistic considerations, the good catalytic activity of 2–5 can be associated with the hydrophilicity of the sulfonate groups. This can activate the water molecule toward its important role as a promoter/catalyst for proton-shift steps involved in the formation of hydroxyl radicals from hydrogen peroxide [50], with a key role in the mechanism of the alkane oxidation.

The participation of the alkylhydroperoxide ROOH species was proved [59–65] by the increase in the amount of ROH and consequent decrease of R_(-H)=O when the final reaction solution was treated with PPh₃ prior to the GC analysis (Table S3, Supplementary Materials).

Moreover, the promoting effect of pyridine can result from the assistance on the proton-transfer steps involved in the formation of the hydroxyl radical [50,59–63] from H₂O₂, whereas the role of the acid additive can be associated with the activation of the metal center by further unsaturation upon ligand protonation, the enhancement of oxidative properties of metal complexes, the stabilization of oxidants, and the promotion of peroxy (or hydroperoxo)-complex formation as indicated in previous cases [37,48,76,77].

For further screening of the hydrocarbon substrates and the scope of our system, the most promising catalyst 3 without any additive was used. Cyclohexane and cyclohexene were successfully transformed employing our catalytic system, thus showing its versatility. The obtained results are summarized in Table 6.

Table 6. Scope of the peroxidative hydrocarbon oxidation employing catalyst **3** ^a.

Entry	Time (h)	Substrate	Yield ^b , %	Selectivity ^c	TON ^d
1	2	Cyclohexane	20	22:78	50
2	4		20	24:76	50
3	8		20	27:73	50
4	24		20	32:68	50
5	32		20	33:67	50
6	2	Cyclohexene	15	8:36:44:4:8	50
7	4		15	7:40:39:5:9	50
8	8		15	6:45:36:5:8	50
9	24		15	1:49:34:8:8	50
10	32		15	0:48:32:10:9	50

^a Reaction conditions: substrate (0.25 M), complex **3** (10^{-3} M), H₂O₂ (1.2 M) in acetonitrile at 60 °C; total volume of reaction mixture is 10 mL. ^b Amounts of oxygenate products were determined after reduction of the aliquots with solid PPh₃ (for this method, see references [61–65]). ^c Cyclohexanone:cyclohexanol and cyclohexene oxide:2-cyclohexen-1-one:2-cyclohexen-1-ol:*cis*-1,2-cyclohexanediol:*trans*-1,2-cyclohexanediol ratio (for reactions with cyclohexane and cyclohexene, respectively). ^d Turnover number of the catalyst (sum of moles of all products per mole of **3**).

In the peroxidative oxidation of cyclohexane, compound **3** leads to a 20% yield, based on the substrate, after 2 h of reaction time with a ketone/alcohol ratio of approximately 20:80 (Table 6, entry 1). As it was observed when cyclooctane was used without any additive, longer reaction times resulted in yield preservation, but a loss on the selectivity until approximately 30:70, after 32 h of reaction time (Table 6).

Overall product yield decreased in the peroxidative oxidation of the alkene (15% based on cyclohexene, after 2 h of reaction time). At 2 h of reaction time, the ratios of cyclohexene oxide:2-cyclohexen-1-one:2-cyclohexen-1-ol:*cis*-1,2-cyclohexanediol:*trans*-1,2-cyclohexanediol were 7:36:44:5:8 (Table 6, entry 6). As in the previous cases, the reaction followed the same trend, not only in terms of yield but also in selectivity, over the reaction time.

3. Materials and Methods

All the reagents and solvents were purchased from commercial sources and used as received. The water used for all preparations and analyses was double-distilled and deionized. Elemental analyses were performed by the Microanalytical Service of the Instituto Superior Técnico (Lisbon, Portugal). FT-IR spectra were recorded in the 400–4000 cm⁻¹ region on a Bruker Vertex 70 spectrophotometer (Bruker Optik GmbH, Ettlingen, Germany) with samples as KBr discs. The ¹H NMR spectra were recorded at room temperature on a Bruker Avance II + 300 (UltraShield™ Magnet) spectrometer (Bruker BioSpin AG, Fällanden, Switzerland). Chromatographic measurements were carried out in a Perkin-Elmer Clarus 500 gas chromatograph (PerkinElmer Inc., Shelton, CT, USA) with a BP-20 capillary column (SGE). The parameters of the column are 30 m × 0.32 mm × 25 μm and Helium was used as the carrier gas (1 mL per minute constant flow).

3.1. Synthesis of H₂L (1)

To a hot and stirred water solution (10 mL) of 2-aminobenzenesulfonic acid (0.692 g, 4.0 mmol) was added dropwise a methanol solution (20 mL) of salicylaldehyde (0.488 g, 4.0 mmol). The resulting yellow solution was filtered and kept at room temperature overnight. After one day, yellow crystals suitable for X-ray diffraction analysis formed and the crystals were collected by filtration and washed with methanol. Yield 1.022 g (92%). Anal. calcd. for C₁₃H₁₁NO₄S (277.29): C 56.31, H 4.00, N 5.05; found: C 56.21, H 4.03, N 5.08. FT-IR (cm⁻¹, KBr): ν(OH), 3445br; ν(N–H), 2919br; ν(C=N), 1638s;

$\nu(\text{C-O})$, 1233s; $\nu(\text{sulfonate})$, 1376s, 1171s, 763m. $^1\text{H NMR}$ (300 MHz, $\text{DMSO-}d_6$) δ values (ppm): 10.69 (br, N-H); 10.26 (s, CH=N); 6.91–7.92 (m, 8-Ar-H). $^{13}\text{C NMR}$ (75.468 MHz) in $\text{DMSO-}d_6$, internal TMS, δ (ppm): 116.8 (Ar-H), 120.1 (Ar-H), 127.6 (Ar-C), 129.0 (Ar-C), 130.8 (Ar-C), 135.4 (Ar-C), 136.5 (Ar-C), 137.4 (Ar-C), 139.4 (Ar-C), 140.1 (Ar-C-SO₃), 162.2 (Ar-C-OH), 164.1 (N=C).

3.2. Synthesis of $[\text{Cu}(\text{L})(\text{py})(\text{EtOH})]$ (2)

To a hot and stirred ethanol suspension (10 mL) of **1** (0.277 g, 1.0 mmol) was added dropwise an ethanol solution (5 mL) of pyridine (0.316 g, 4.0 mmol) affording a clear orange solution. Then, an ethanol solution (5 mL) of $\text{CuCl}_2 \cdot 2\text{H}_2\text{O}$ (0.170 g, 1.0 mmol) was added dropwise to obtain a dark green solution. The solution was filtered and kept at room temperature. After two days, green crystals suitable for X-ray diffraction analysis formed and the crystals were collected by filtration and washed with ethanol. Yield: 0.362 g (78%). Anal. calcd. for $\text{C}_{20}\text{H}_{20}\text{CuN}_2\text{O}_5\text{S}$ (463.98): C 51.77, H 4.34, N 6.04; found C 51.75, H 4.26, N 6.07. FT-IR (cm^{-1} , KBr): $\nu(\text{C=N})$, 1606; $\nu(\text{C-O})$, 1283s; $\nu(\text{sulfonate})$, 1383m, 1174s, 764m.

3.3. Synthesis of $[\text{Cu}(\text{L})(\text{bipy})] \cdot \text{MeOH}$ (3)

To a methanol solution (40 mL) of **2** (0.232 g, 0.5 mmol) was added dropwise a methanol solution (10 mL) of 2,2'-bipyridine (0.156 g, 1.0 mmol) affording a dark green solution. After a few hours, a dark green crystalline compound suitable for X-ray diffraction analysis formed and was collected by filtration and washed with methanol. Yield: 0.235 g (89%). Anal. calcd. for $\text{C}_{24}\text{H}_{21}\text{CuN}_3\text{O}_5\text{S}$ (527.04): C 54.69, H 4.02, N 7.97; found C 54.80, H 4.06, N 7.91. FT-IR (cm^{-1} , KBr): $\nu(\text{C=N})$, 1611; $\nu(\text{C-O})$, 1294m; $\nu(\text{sulfonate})$, 1386m, 1181s, 769m.

3.4. Synthesis of $[\text{Cu}_2(\text{L})_2(\mu\text{-pyr})(\text{MeOH})_2]$ (4)

To a methanol solution (15 mL) of **2** (0.232 g, 0.5 mmol) was added dropwise a methanol solution (5 mL) of pyrazine (0.080 g, 1.0 mmol) affording a dark green solution. After one day, a dark green crystalline compound suitable for X-ray diffraction analysis formed and was collected by filtration and washed with methanol. Yield: 0.177g (86%). Anal. calcd. for $\text{C}_{32}\text{H}_{30}\text{Cu}_2\text{N}_4\text{O}_{10}\text{S}_2$ (821.80): C 46.77, H 3.68, N 6.82; found C 46.87, H 3.76, N 6.75. FT-IR (cm^{-1} , KBr): $\nu(\text{C=N})$, 1613s; $\nu(\text{C-O})$, 1264m; $\nu(\text{sulfonate})$, 1382m, 1160s, 770m.

3.5. Synthesis of $[\text{Cu}_2(\text{L})_2(\mu\text{-pip})(\text{MeOH})_2]$ (5)

To a methanol solution (40 mL) of **2** (0.232 g, 0.5 mmol) was added dropwise a methanol solution (10 mL) of piperazine (0.086 g, 1.0 mmol) affording a dark green solution. After a few hours, a dark green crystalline compound suitable for X-ray diffraction analysis formed and was collected by filtration and washed with methanol. Yield: 0.176 g (85%). Anal. calcd. for $\text{C}_{32}\text{H}_{36}\text{Cu}_2\text{N}_4\text{O}_{10}\text{S}_2$ (827.85): C 46.43, H 4.38, N 6.77; found C 46.55, H 4.28, N 6.73. FT-IR (cm^{-1} , KBr): $\nu(\text{C=N})$, 1612s; $\nu(\text{C-O})$, 1248m; $\nu(\text{sulfonate})$, 1385m, 1176s, 756m.

3.6. Crystal Structure Determinations

X-ray quality crystals of all compounds were immersed in cryo-oil, mounted in a Nylon loop, and measured at a temperature of 150 K (**1**, **2**, and **5**) or 296 K (**3** and **4**). Intensity data were collected using a Bruker AXS-KAPPA APEX II or a Bruker APEX-II PHOTON 100 diffractometer (Bruker AXS GmbH, Karlsruhe, Germany) with graphite monochromated Mo-K α (λ 0.71073) radiation. Data were collected using omega scans of 0.5° per frame and a full sphere of data was obtained. Cell parameters were retrieved using Bruker SMART software and refined using Bruker SAINT [78] on all the observed reflections. Absorption corrections were applied using SADABS [78]. Structures were solved by direct methods using the SHELXS-97 package [79,80] and refined with SHELXL-97 [79,80]. Calculations were performed using the WinGX System, Version 1.80.03 [81]. The hydrogen atoms attached to carbon

atoms and to nitrogen atoms were inserted at geometrically calculated positions and included in the refinement using the riding-model approximation; Uiso(H) were defined as 1.2 Ueq of the parent nitrogen atoms or the carbon atoms for phenyl and methylene residues and 1.5 Ueq of the parent carbon atoms for the methyl groups. The hydrogen atoms of the hydroxide (in all structures but **5**) were located from the final difference Fourier map, and the isotropic thermal parameters were set at 1.5 times the average thermal parameters of the belonging oxygen atoms. Least-square refinements with anisotropic thermal motion parameters for all the non-hydrogen atoms and isotropic for the remaining atoms were employed. Crystallographic data are summarized in Table S4 (Supplementary Materials).

3.7. Hydrocarbon Oxidation Studies

The catalytic oxidation reactions of hydrocarbons were carried out in MeCN solvent (total volume of 10.0 mL) in thermostated Pyrex round-bottom vessels and in open atmosphere, at 60 °C. The catalyst was used and introduced into the reaction mixture in the form of a stock solution in acetonitrile prepared by dissolving the catalyst (**2–5**) in acetonitrile. The substrate and promoter (if any) were then added in this order and the reaction started with the addition of 50% aqueous hydrogen peroxide in a portion. (CAUTION: the combination of air or molecular oxygen and H₂O₂ with organic compounds at elevated temperatures may be explosive!) The initial concentrations of hydrocarbon, catalyst, H₂O₂, and promoter (if used) were 0.25 M, 10^{−3} M per copper, 1.2 M, and 0.072 M, respectively. Solutions were analyzed by GC after the addition of nitromethane, as a standard compound, and the attribution of peaks was made by comparison with chromatograms of authentic samples.

GC analyses in the presence and in the absence of PPh₃ were carried out, and it was found that the oxygenation of cycloalkanes resulted in the formation of the corresponding cycloalkyl hydroperoxides as the main primary products as expected, according to the method developed by Shul'pin [59–65]. For a precise determination of the product concentrations, only data obtained after the reduction of the reaction sample with PPh₃ were typically used, taking into account that the original reaction mixture contained the three products: cycloalkyl hydroperoxide (as the primary product), ketone, and alcohol. When used, the oxygen radical trap [37] diphenylamine (Ph₂NH) and the carbon radical trap [37] bromotrichloromethane (CBrCl₃) were applied in a stoichiometric amount relatively to the oxidant and substrate, respectively.

4. Conclusions

By taking advantage of the chelating capacity of the acyclic Schiff base *o*-[(*o*-hydroxyphenyl)methylideneamino]benzenesulfonic acid H₂L (**1**), as well as of the H-bonding formation ability of the non-coordinating sulfonate group and in the presence of an *N*-heterocyclic base, namely, pyridine (py), 2,2'-bipyridine (bipy), pyrazine (pyr), or piperazine (pip), four new copper(II) complexes, that is, [Cu(L)(py)(EtOH)] (**2**), [Cu(L)(bipy)]·MeOH (**3**), [Cu₂(L)₂(μ-pyr)(MeOH)₂] (**4**), and [Cu₂(L)₂(μ-pip)(MeOH)₂] (**5**) were synthesized. The crystal lattices of all compounds, with the exception of **3**, were stabilized by a number of non-covalent H-bonding interactions and generated interesting H-bonded polymeric networks, namely, a zigzag 1D chain (in **1**), a linear 1D (in **2**), a hacksaw double chain 1D (in **4**), and a 2D motif (in **5**). Double coordination of 2,2-bipyridine diminished the possibility of solvent coordination and no dimensionality was formed in the crystal lattice of **3**.

These copper(II) complexes (**2–5**) catalyzed the peroxidative hydrocarbon (cycloalkane and cycloalkene) oxidation under mild conditions either in the absence or presence of an additive. As a model system, we used cyclooctane and hydrogen peroxide as substrate and oxidant, respectively. The presence of a basic or an acid promoter usually enhanced the catalytic activity.

The best activity was exhibited, in general, by the mononuclear compounds, where **3** was the most effective one, either without any promoter (20% max. yield) or in the presence of pyridine (26% max. yield), whereas **2** displayed the highest activity in the presence of HNO₃ (35% max. yield). For each complex, although the reactions were significantly faster with pyridine, the best product

yields were achieved with the acid additive. Other substrates, namely, cyclohexane and cyclohexene, were also oxidized catalytically with complex **3** into the oxidized products in overall 20% and 15% yields, respectively, without any additive, attesting to the versatility of our catalytic system.

Our studies with diphenylamine and bromotrichloromethane showed that the cyclooctane oxidation reaction appears to proceed mainly via a non-free radical pathway for short reaction times, although over time a free radical mechanism involving oxygen- and carbon-centered radicals becomes relevant. Such a curious behavior does not seem to have been recognized earlier and deserves to be tested not only in already known catalytic systems but also in novel ones.

The synthetic methodologies based on the addition (for the synthesis of **2**) or substitution of pyridine for a *N*-heterocyclic base (2,2'-bipyridine, pyrazine, or piperazine for the synthesis of **3–5**) to produce mono- and dinuclear copper systems in alcoholic medium provide easy synthetic procedures in comparison with other approaches for the syntheses of copper(II) complexes which are active for catalytic alkane oxidation [44,45,47,48,51,52].

In summary, a simple protocol for the synthesis of four effective catalysts is presented. However, detailed mechanistic studies—which include the kinetics of H₂O₂ decomposition, the influence of the O₂ atmosphere in the catalytic activity, electron paramagnetic resonance (EPR) measurements, the use of dimethylsulfoxide as selective hydroxyl radical scavenger, and (Density Functional Theory) DFT calculations to disclose the active species and understand the mechanism—are under progress and should be the subject of a further publication.

Supplementary Materials: The following are available online at <http://www.mdpi.com/2304-6740/7/2/17/s1>, H-Bonded networks in **1–5**, **Figure S1:** Idealized capped stick presentation of the H-bonds in **1** with partially atom labelling scheme, **Figure S2:** Idealized capped stick presentation of the H-bonded zigzag 1D chain in **1**, **Figure S3:** Idealized capped stick presentations of the H-bonded linear 1D in **2**, double chain 1D in **4**, and 2D motif in **5**, **Table S1:** Geometries (distances in Å) and angles in (°) of the H-bonds in **1–5**, **Table S2:** Tests concerning the oxidation of cyclooctane in the presence of H₂L (**1**) and in the absence of any metal catalyst (blank tests), **Table S3:** Results obtained before the reduction with PPh₃ of the aliquots of the oxidation of cyclooctane catalyzed by **3**, **Table S4:** Crystallographic data for **1–5**, **Table S5:** Effect of the presence of diphenylamine on the oxidation of cyclooctane catalyzed by **3**, **Table S6:** Effect of the presence of bromotrichloromethane on the oxidation of cyclooctane catalyzed by **3**. CCDC 958691–958695 for **1–5**, respectively, contain the supplementary crystallographic data for this paper. These data can be obtained free of charge from the Cambridge Crystallographic Data Centre at http://www.ccdc.cam.ac.uk/data_request/cif or from the Cambridge Crystallographic Data Centre, 12 Union Road, Cambridge CB2 1EZ, UK; fax: (+44) 1223 336 033; or e-mail: deposit@ccdc.cam.ac.uk.

Author Contributions: Conceptualization, S.H., M.F.C.G.d.S. and A.J.L.P.; Methodology, S.H., B.G.M.R. and A.K.; Software, S.H., B.G.M.R. and M.F.C.G.d.S.; Validation, S.H., B.G.M.R. and A.K.; Formal Analysis, S.H. and B.G.M.R.; Investigation, S.H. and B.G.M.R.; Resources, S.H., B.G.M.R. and A.K.; Data Curation, S.H. and B.G.M.R.; Writing—Original Draft Preparation, S.H. and B.G.M.R.; Writing—Review&Editing, S.H., M.F.C.G.d.S. and A.J.L.P.; Visualization, S.H.; Supervision, S.H., M.F.C.G.d.S. and A.J.L.P.; Project Administration, S.H. and A.J.L.P.; Funding Acquisition, S.H., B.G.M.R., A.K. and A.J.L.P.

Funding: The work was partially supported by the Fundação para a Ciência e a Tecnologia (FCT), Portugal, and its PPCDT program (FEDER funded) through the research projects PTDC/QEQ-QIN/3967/2014 and UID/QUI/00100/2013. S.H. and A.K. acknowledge FCT for the postdoctoral grants SFRH/BPD/78264/2011 and SFRH/BPD/76192/2011. S.H. also acknowledges FCT and IST (Instituto Superior Tecnico, Lisbon, Portugal) for his working contract (Contract No. IST-ID/103/2018). B.G.M.R. is grateful to the Group V of Centro de Química Estrutural and the FCT, for the fellowships BL/CQE-2012-026, BL/CQE-2013-010 and the PhD fellowship under the CATSUS PhD program (SFRH/BD/52370/2013).

Acknowledgments: The authors acknowledge the Portuguese NMR Network (IST-UTL Center, Lisbon, Portugal) for providing access to the NMR facility.

Conflicts of Interest: The authors declare no conflict of interest.

References

1. Hazra, S.; Martins, N.M.R.; Kuznetsov, M.L.; Guedes da Silva, M.F.C.; Pombeiro, A.J.L. Flexibility and lability of a phenyl ligand in hetero-organometallic 3d metal–Sn(IV) compounds and their catalytic activity in Baeyer–Villiger oxidation of cyclohexanone. *Dalton Trans.* **2017**, *46*, 13364–13375. [[CrossRef](#)] [[PubMed](#)]
2. Hazra, S.; Chakraborty, P.; Mohanta, S. Heterometallic Copper(II)–Tin(II/IV) Salts, Cocrystals, and Salt Cocrystals: Selectivity and Structural Diversity Depending on Ligand Substitution and the Metal Oxidation State. *Cryst. Growth Des.* **2016**, *16*, 3777–3790. [[CrossRef](#)]
3. Hazra, S.; Meyrelles, R.; Charmier, A.J.; Rijo, P.; Guedes da Silva, M.F.C.; Pombeiro, A.J.L. N–H···O and N–H···Cl supported 1D chains of heterobimetallic Cu^{II}/Ni^{II}–Sn^{IV} cocrystals. *Dalton Trans.* **2016**, *45*, 17929–17938. [[CrossRef](#)] [[PubMed](#)]
4. Hazra, S.; Titiš, J.; Valigura, D.; Boca, R.; Mohanta, S. Bis-phenoxido and bis-acetato bridged heteronuclear {Co^{III}Dy^{III}} single molecule magnets with two slow relaxation branches. *Dalton Trans.* **2016**, *45*, 7510–7520. [[CrossRef](#)] [[PubMed](#)]
5. Hazra, S.; Bhattacharya, S.; Singh, M.K.; Carrella, L.; Rentschler, E.; Weyhermueller, T.; Rajaraman, G.; Mohanta, S. Syntheses, Structures, Magnetic Properties, and Density Functional Theory Magneto-Structural Correlations of Bis(μ-phenoxo) and Bis(μ-phenoxo)-μ-acetate/Bis(μ-phenoxo)-bis(μ-acetate) Dinuclear Fe^{III}Ni^{II}Compounds. *Inorg. Chem.* **2013**, *52*, 12881–12892. [[CrossRef](#)]
6. Hazra, S.; Sasmal, S.; Fleck, M.; Grandjean, F.; Sougrati, M.T.; Ghosh, M.; Harris, T.D.; Bonville, P.; Long, G.J.; Mohanta, S. Slow magnetic relaxation and electron delocalization in an $S = 9/2$ iron(II/III) complex with two crystallographically inequivalent iron sites. *J. Chem. Phys.* **2011**, *134*, 174507. [[CrossRef](#)] [[PubMed](#)]
7. Kahn, O. Chemistry and Physics of Supramolecular Magnetic Materials. *Acc. Chem. Res.* **2000**, *33*, 647–657. [[CrossRef](#)]
8. Zhang, D.; Wang, H.; Chen, Y.; Ni, Z.-H.; Tian, L.; Jiang, J. Hydrogen-Bond Directed Cyanide-Bridged Molecular Magnets Derived from Polycyanidometalates and Schiff Base Manganese(III) Compounds: Synthesis, Structures, and Magnetic Properties. *Inorg. Chem.* **2009**, *48*, 11215–11225. [[CrossRef](#)]
9. Sasmal, S.; Hazra, S.; Kundu, P.; Majumder, S.; Aliaga-Alcalde, N.; Ruiz, E.; Mohanta, S. Magneto-Structural Correlation Studies and Theoretical Calculations of a Unique Family of Single End-to-End Azide-Bridged Ni^{II}₄ Cyclic Clusters. *Inorg. Chem.* **2010**, *49*, 9517–9526. [[CrossRef](#)]
10. Redshaw, C.; Elsegood, M.R.J.; Frese, J.W.A.; Ashby, S.; Chao, Y.; Mueller, A. Cellular uptake studies of two hexanuclear, carboxylate bridged, zinc ring structures using fluorescence microscopy. *Chem. Commun.* **2012**, *48*, 6627–6629. [[CrossRef](#)]
11. Yang, X.; Jones, R.A. Anion Dependent Self-Assembly of “Tetra-Decker” and “Triple-Decker” Luminescent Tb(III) Salen Complexes. *J. Am. Chem. Soc.* **2005**, *127*, 7686–7687. [[CrossRef](#)]
12. Liao, S.; Yang, X.; Jones, R.A. Self-Assembly of Luminescent Hexanuclear Lanthanide Salen Complexes. *Cryst. Growth Des.* **2012**, *12*, 970–974. [[CrossRef](#)]
13. Wu, J.-Q.; Pan, L.; Li, Y.-G.; Liu, S.-R.; Li, Y.-S. Synthesis, Structural Characterization, and Olefin Polymerization Behavior of Vanadium(III) Complexes Bearing Tridentate Schiff Base Ligands. *Organometallics* **2009**, *28*, 1817–1825. [[CrossRef](#)]
14. Bania, K.K.; Bharali, D.; Viswanathan, B.; Deka, R.C. Enhanced Catalytic Activity of Zeolite Encapsulated Fe(III)–Schiff-Base Complexes for Oxidative Coupling of 2-Naphthol. *Inorg. Chem.* **2012**, *51*, 1657–1674. [[CrossRef](#)] [[PubMed](#)]
15. Handa, S.; Gnanadesikan, V.; Matsunaga, S.; Shibasaki, M. Heterobimetallic Transition Metal/Rare Earth Metal Bifunctional Catalysis: A Cu/Sm/Schiff Base Complex for *Syn*-Selective Catalytic Asymmetric Nitro-Mannich Reaction. *J. Am. Chem. Soc.* **2010**, *132*, 4925–4934. [[CrossRef](#)] [[PubMed](#)]
16. Burkhardt, A.; Spielberg, E.T.; Görls, H.; Plass, W. Chiral Tetranuclear μ₃-Alkoxo-Bridged Copper(II) Complex with 2 + 4 Cubane-Like Cu₄O₄ Core Framework and Ferromagnetic Ground State. *Inorg. Chem.* **2008**, *47*, 2485–2493. [[CrossRef](#)] [[PubMed](#)]
17. Redshaw, C.; Elsegood, M.R.J. Novel organoaluminium (and gallium) carboxylate-bridged ring systems. *Chem. Commun.* **2001**, *0*, 2016–2017. [[CrossRef](#)]
18. Puterová, Z.; Valentová, J.; Bojková, Z.; Kožíšek, J.; Devínský, F. Synthesis, crystal structure and antiradical effect of copper(II) Schiff base complexes containing five-, six- and unusual seven-membered rings. *Dalton Trans.* **2011**, *40*, 1484–1490. [[CrossRef](#)] [[PubMed](#)]

19. Hazra, S.; Mukherjee, S.; da Silva, M.F.; Pombeiro, A.J. A cyclic tetranuclear cuboid type copper(II) complex doubly supported by cyclohexane-1,4-dicarboxylate: Molecular and supramolecular structure and cyclohexane oxidation activity. *RSC Adv.* **2014**, *4*, 48449–48457. [[CrossRef](#)]
20. Hazra, S.; Karmakar, A.; Guedes da Silva, M.F.C.; Dlhán, L.; Boca, R.; Pombeiro, A.J.L. Sulfonated Schiff base dinuclear and polymeric copper(II) complexes: Crystal structures, magnetic properties and catalytic application in Henry reaction. *New J. Chem.* **2015**, *39*, 3424–3434. [[CrossRef](#)]
21. Hazra, S.; Karmakar, A.; Guedes da Silva, M.F.C.; Dlhán, L.; Boca, R.; Pombeiro, A.J.L. Dinuclear based polymeric copper(II) complexes derived from a Schiff base ligand: Effect of secondary bridging moieties on geometrical orientations and magnetic properties. *Inorg. Chem. Commun.* **2014**, *46*, 113–117. [[CrossRef](#)]
22. Hazra, S.; Guedes da Silva, M.F.C.; Karmakar, A.; Pombeiro, A.J.L. 1D hacksaw chain bipyridine–sulfonate Schiff base-dicopper(II) as a host for variable solvent guests. *RSC Adv.* **2015**, *5*, 28070–28079. [[CrossRef](#)]
23. Ribeiro, A.P.; Martins, L.M.; Hazra, S.; Pombeiro, A.J. Catalytic oxidation of cyclohexane with hydrogen peroxide and a tetracopper(II) complex in an ionic liquid. *Compt. Rend. Chim.* **2015**, *18*, 758–765. [[CrossRef](#)]
24. Hazra, S.; Martins, L.M.; Guedes da Silva, M.F.C.; Pombeiro, A.J.L. Sulfonated Schiff base copper(II) complexes as efficient and selective catalysts in alcohol oxidation: Syntheses and crystal structures. *RSC Adv.* **2015**, *5*, 90079–90088. [[CrossRef](#)]
25. Martins, L.M.; Hazra, S.; Guedes da Silva, M.F.C.; Pombeiro, A.J.L. A sulfonated Schiff base dimethyltin(IV) coordination polymer: Synthesis, characterization and application as a catalyst for ultrasound- or microwave-assisted Baeyer–Villiger oxidation under solvent-free conditions. *RSC Adv.* **2016**, *6*, 78225–78233. [[CrossRef](#)]
26. Hazra, S.; Paul, A.; Sharma, G.; Koch, B.; Guedes da Silva, M.F.C.; Pombeiro, A.J.L. Sulfonated Schiff base Sn(IV) complexes as potential anticancer agents. *J. Inorg. Biochem.* **2016**, *162*, 83–95. [[CrossRef](#)] [[PubMed](#)]
27. Hazra, S.; Martins, L.M.; Guedes da Silva, M.F.C.; Pombeiro, A.J.L. Sulfonated Schiff base dimeric and polymeric copper(II) complexes: Temperature dependent synthesis, crystal structure and catalytic alcohol oxidation studies. *Inorg. Chim. Acta* **2017**, *455*, 549–556. [[CrossRef](#)]
28. Hazra, S.; Ribeiro, A.P.C.; Guedes da Silva, M.F.C.; Nieto de Castro, C.A.; Pombeiro, A.J.L. Syntheses and crystal structures of benzene-sulfonate and -carboxylate copper polymers and their application in the oxidation of cyclohexane in ionic liquid under mild conditions. *Dalton Trans.* **2016**, *45*, 13957–13968. [[CrossRef](#)]
29. Paul, A.; Hazra, S.; Sharma, G.; Guedes da Silva, M.F.C.; Koch, B.; Pombeiro, A.J.L. Unfolding biological properties of a versatile dicopper(II) precursor and its two mononuclear copper(II) derivatives. *J. Inorg. Biochem.* **2017**, *174*, 25–36. [[CrossRef](#)]
30. Othmer, D.F. *Kirk-Othmer Concise Encyclopedia of Chemical Technology*, 5th ed.; 2nd Volume Set; John Wiley & Sons, Inc.: Hoboken, NJ, USA, 2007.
31. Sutradhar, M.; Shvydkiy, N.V.; Guedes da Silva, M.F.C.; Kirillova, M.V.; Kozlov, Y.N.; Pombeiro, A.J.L.; Shul'pin, G.B. A new binuclear oxovanadium(V) complex as a catalyst in combination with pyrazinecarboxylic acid(PCA) for efficient alkane oxygenation by H₂O₂. *Dalton Trans.* **2013**, *42*, 11791–11803. [[CrossRef](#)]
32. Sutradhar, M.; Kirillova, M.V.; Guedes da Silva, M.F.C.; Martins, L.M.D.R.S.; Pombeiro, A.J.L. A Hexanuclear Mixed-Valence Oxovanadium(IV,V) Complex as a Highly Efficient Alkane Oxidation Catalyst. *Inorg. Chem.* **2012**, *51*, 11229–11232. [[CrossRef](#)] [[PubMed](#)]
33. Stahl, S.S.; Labinger, J.A.; Bercaw, J.E. Homogeneous Oxidation of Alkanes by Electrophilic Late Transition Metals. *Angew. Chem. Int. Ed.* **1998**, *37*, 2180–2192. [[CrossRef](#)]
34. Mokaya, R.; Poliakov, M. A cleaner way to nylon? *Nature* **2005**, *437*, 1243–1244. [[CrossRef](#)] [[PubMed](#)]
35. Ullmann, F. *Ullmann's Encyclopedia of Industrial Chemistry*, 6th ed.; Wiley-VCH: Weinheim, Germany, 2002.
36. Schuchardt, U.; Cardoso, D.; Sercheli, R.; Pereira, R.; da Cruz, R.S.; Guerreiro, M.C.; Mandelli, D.; Spinacé, E.V.; Pires, E.L. Cyclohexane oxidation continues to be a challenge. *Appl. Catal. A: Gen.* **2001**, *211*, 1–17. [[CrossRef](#)]
37. Slaughter, L.M.; Collman, J.P.; Eberspacher, T.A.; Brauman, J.I. Radical Autoxidation and Autogenous O₂ Evolution in Manganese–Porphyrin Catalyzed Alkane Oxidations with Chlorite. *Inorg. Chem.* **2004**, *43*, 5198–5204. [[CrossRef](#)] [[PubMed](#)]
38. Lane, B.S.; Burgess, K. Metal-Catalyzed Epoxidations of Alkenes with Hydrogen Peroxide. *Chem. Rev.* **2003**, *103*, 2457–2474. [[CrossRef](#)] [[PubMed](#)]

39. Grigoropoulou, G.; Clark, J.H.; Elings, J.A. Recent developments on the epoxidation of alkenes using hydrogen peroxide as an oxidant. *Green Chem.* **2003**, *5*, 1–7. [[CrossRef](#)]
40. Muzart, J. Pd-mediated epoxidation of olefins. *J. Mol. Catal. A* **2007**, *276*, 62–72. [[CrossRef](#)]
41. Díaz-Requejo, M.M.; Pérez, P.J. Coinage Metal Catalyzed C–H Bond Functionalization of Hydrocarbons. *Chem. Rev.* **2008**, *108*, 3379–3394. [[CrossRef](#)]
42. Crabtree, R.H. Editorial: Introduction to Selective Functionalization of C–H Bonds. *Chem. Rev.* **2010**, *110*, 575. [[CrossRef](#)]
43. Nesterov, D.S.; Nesterova, O.V.; Pombeiro, A.J.L. Homo- and heterometallic polynuclear transition metal catalysts for alkane C–H bonds oxidative functionalization: Recent advances. *Coord. Chem. Rev.* **2018**, *355*, 199–222. [[CrossRef](#)]
44. Silva, T.F.S.; Alegria, E.C.B.A.; Martins, L.M.D.R.S.; Pombeiro, A.J.L. Half-Sandwich Scorpionate Vanadium, Iron and Copper Complexes: Synthesis and Application in the Catalytic Peroxidative Oxidation of Cyclohexane under Mild Conditions. *Adv. Synth. Catal.* **2008**, *350*, 706–716. [[CrossRef](#)]
45. Silva, T.F.; Mishra, G.S.; da Silva, M.F.; Wanke, R.; Martins, L.M.; Pombeiro, A.J. Cu^{II} complexes bearing the 2,2,2-tris(1-pyrazolyl)ethanol or 2,2,2-tris(1-pyrazolyl)ethyl methanesulfonate scorpionates. X-Ray structural characterization and application in the mild catalytic peroxidative oxidation of cyclohexane. *Dalton Trans.* **2009**, 9207–9215. [[CrossRef](#)]
46. Da Silva, J.A.L.; da Silva, J.J.R.F.; Pombeiro, A.J.L. Oxovanadium complexes in catalytic oxidations. *Coord. Chem. Rev.* **2011**, *255*, 2232–2248. [[CrossRef](#)]
47. Kirillov, A.M.; Kopylovich, M.N.; Kirillova, M.V.; Haukka, M.; Guedes da Silva, M.F.C.; Pombeiro, A.J.L. Multinuclear Copper Triethanolamine Complexes as Selective Catalysts for the Peroxidative Oxidation of Alkanes under Mild Conditions. *Angew. Chem. Int. Ed.* **2005**, *44*, 4345–4349. [[CrossRef](#)] [[PubMed](#)]
48. Kirillov, A.M.; Kopylovich, M.N.; Kirillova, M.V.; Karabach, Y.Y.; Haukka, M.; Guedes da Silva, M.F.C.; Pombeiro, A.J.L. Mild Peroxidative Oxidation of Cyclohexane Catalyzed by Mono-, Di-, Tri-, Tetra- and Polynuclear Copper Triethanolamine Complexes. *Adv. Synth. Catal.* **2006**, *348*, 159–174. [[CrossRef](#)]
49. Nicola, C.D.; Karabach, Y.Y.; Kirillov, A.M.; Monari, M.; Pandolfo, L.; Pettinari, C.; Pombeiro, A.J.L. Supramolecular Assemblies of Trinuclear Triangular Copper(II) Secondary Building Units through Hydrogen Bonds. Generation of Different Metal–Organic Frameworks, Valuable Catalysts for Peroxidative Oxidation of Alkanes. *Inorg. Chem.* **2007**, *46*, 221–230. [[CrossRef](#)]
50. Kuznetsov, M.; Pombeiro, A.J.L. Radical Formation in the [MeReO₃]-Catalyzed Aqueous Peroxidative Oxidation of Alkanes: A Theoretical Mechanistic Study. *Inorg. Chem.* **2009**, *48*, 307–318. [[CrossRef](#)]
51. Roy, P.; Manassero, M. Tetranuclear copper(II)–Schiff-base complexes as active catalysts for oxidation of cyclohexane and toluene. *Dalton Trans.* **2010**, *39*, 1539–1545. [[CrossRef](#)]
52. Dronova, M.S.; Bilyachenko, A.N.; Yalymov, A.I.; Kozlov, Y.N.; Shul’pina, L.S.; Korlyukov, A.A.; Arkhipov, D.E.; Levitsky, M.M.; Shubina, E.S.; Shul’pin, G.B. Solvent-controlled synthesis of tetranuclear cage-like copper(II) silsesquioxanes. Remarkable features of the cage structures and their high catalytic activity in oxidation with peroxides. *Dalton Trans.* **2014**, *43*, 872–882. [[CrossRef](#)]
53. Rocha, B.G.M.; Kuznetsov, M.L.; Kozlov, Y.N.; Pombeiro, A.J.L.; Shul’pin, G.B. Simple soluble Bi(III) salts as efficient catalysts for the oxidation of alkanes with H₂O₂. *Catal. Sci. Technol.* **2015**, *5*, 2174–2187. [[CrossRef](#)]
54. Shul’pin, G.B.; Gradinaru, J.; Kozlov, Y.N. Alkane hydroperoxidation with peroxides catalyzed by copper complexes. *Org. Biomol. Chem.* **2003**, *1*, 3611–3617. [[CrossRef](#)] [[PubMed](#)]
55. Süß-Fink, G.; Gonzalez, L.; Shul’pin, G.B. Alkane oxidation with hydrogen peroxide catalyzed homogeneously by vanadium-containing polyphosphomolybdates. *Appl. Catal. A* **2001**, *217*, 111–117. [[CrossRef](#)]
56. Kirillova, M.V.; Kozlov, Y.N.; Shul’pina, L.S.; Lyakin, O.Y.; Kirillov, A.M.; Talsi, E.P.; Pombeiro, A.J.L.; Shul’pin, G.B. Remarkably fast oxidation of alkanes by hydrogen peroxide catalyzed by a tetracopper(II) triethanolamine complex: Promoting effects of acid co-catalysts and water, kinetic and mechanistic features. *J. Catal.* **2009**, *268*, 26–38. [[CrossRef](#)]
57. Costas, M.; Mehn, M.P.; Jensen, M.P.; Que, L., Jr. Dioxygen Activation at Mononuclear Nonheme Iron Active Sites: Enzymes, Models, and Intermediates. *Chem. Rev.* **2004**, *104*, 939–986. [[CrossRef](#)] [[PubMed](#)]
58. Costas, M.; Chen, K.; Que, L., Jr. Biomimetic nonheme iron catalysts for alkane hydroxylation. *Coord. Chem. Rev.* **2000**, *200–202*, 517–544. [[CrossRef](#)]

59. Shul'pin, G.B. *Transition Metals for Organic Synthesis*, 2nd ed.; Bellera, M., Bolm, C., Eds.; Wiley-VCH: New York, NY, USA, 2004; p. 215.
60. Shul'pin, G.B.; Nizova, G.V. Formation of alkyl peroxides in oxidation of alkanes by H₂O₂ catalyzed by transition metal complexes. *React. Kinet. Catal. Lett.* **1992**, *48*, 333–338. [[CrossRef](#)]
61. Shul'pin, G.B.; Kozlov, Y.N.; Nizova, G.V.; Süß-Fink, G.; Stanislas, S.; Kitaygorodskiy, A.; Kulikova, V.S. Oxidations by the reagent “O₂–H₂O₂–vanadium derivative–pyrazine-2-carboxylic acid”. Part 12.¹Main features, kinetics and mechanism of alkane hydroperoxidation. *J. Chem. Soc. Perkin Trans.* **2001**, *2*, 1351–1371. [[CrossRef](#)]
62. Shul'pin, G.B.; Matthes, M.G.; Romakh, V.B.; Barbosa, M.I.F.; Aoyagi, J.L.T.; Mandelli, D. Oxidations by the system “hydrogen peroxide–[Mn₂L₂O₃][PF₆]₂ (L=1,4,7-trimethyl-1,4,7-triazacyclononane)–carboxylic acid”. Part 10: Co-catalytic effect of different carboxylic acids in the oxidation of cyclohexane, cyclohexanol, and acetone. *Tetrahedron* **2008**, *64*, 2143–2152. [[CrossRef](#)]
63. Shul'pin, G.B. Metal-catalyzed hydrocarbon oxygenations in solutions: The dramatic role of additives: A review. *J. Mol. Catal. A: Chem.* **2002**, *189*, 39–66. [[CrossRef](#)]
64. Shul'pin, G.B. C–H functionalization: Thoroughly tuning ligands at a metal ion, a chemist can greatly enhance catalyst's activity and selectivity. *Dalton Trans.* **2013**, *42*, 12794–12818. [[CrossRef](#)] [[PubMed](#)]
65. Shul'pin, G.B. Selectivity enhancement in functionalization of C–H bonds: A review. *Org. Biomol. Chem.* **2010**, *8*, 4217–4228. [[CrossRef](#)] [[PubMed](#)]
66. Kodera, M.; Shimakoshi, H.; Kano, K. First example of a rigid (μ-oxo-di-μ-acetato) diiron(III) complex with 1,2-bis[2-di(2-pyridyl)methyl-6-pyridyl]ethane; its efficient catalysis for functionalization of alkanes. *Chem. Commun.* **1996**, *0*, 1737–1738. [[CrossRef](#)]
67. Schneider, H.-J.; Müller, W. Selective functionalization of hydrocarbons. 6. Mechanistic and preparative studies on the regio- and stereoselective paraffin hydroxylation with peracids. *J. Org. Chem.* **1985**, *50*, 4609–4615. [[CrossRef](#)]
68. Mikami, Y.; Dhakshinamoorthy, A.; Alvaro, M.; Garcia, H. Superior Performance of Fe(BTC) With Respect to Other Metal-Containing Solids in the N-Hydroxyphthalimide-Promoted Heterogeneous Aerobic Oxidation of Cycloalkanes. *ChemCatChem* **2013**, *5*, 1964–1970. [[CrossRef](#)]
69. Theysen, N.; Leitner, W. Selective oxidation of cyclooctane to cyclootaneone with molecular oxygen in the presence of compressed carbon dioxide. *Chem. Commun.* **2002**, 410–411. [[CrossRef](#)]
70. Dhakshinamoorthy, A.; Primo, A.; Concepcion, P.; Alvaro, M.; Garcia, H. Doped Graphene as a Metal-Free Carbocatalyst for the Selective Aerobic Oxidation of Benzylic Hydrocarbons, Cyclooctane and Styrene. *Chem. Eur. J.* **2013**, *19*, 7547–7554. [[CrossRef](#)]
71. Hu, B.; Zhou, W.; Ma, D.; Liu, Z. Metallo-deuteroporphyrins as catalysts for the oxidation of cyclohexane with air in the absence of additives and solvents. *Catal. Commun.* **2008**, *10*, 83–85. [[CrossRef](#)]
72. Halvagar, M.R.; Solntsev, P.V.; Lim, H.; Hedman, B.; Hodgson, K.O.; Solomon, E.I.; Cramer, C.J.; Tolman, W.B. Hydroxo-Bridged Dicopper(II,III) and -(III,III) Complexes: Models for Putative Intermediates in Oxidation Catalysis. *J. Am. Chem. Soc.* **2014**, *136*, 7269–7272. [[CrossRef](#)]
73. Haack, P.; Kärgel, A.; Greco, C.; Dokic, J.; Braun, B.; Pfaff, F.F.; Mebs, S.; Ray, K.; Limberg, C. Access to a Cu^{II}–O–Cu^{II} Motif: Spectroscopic Properties, Solution Structure, and Reactivity. *J. Am. Chem. Soc.* **2013**, *135*, 16148–16151. [[CrossRef](#)]
74. Mirica, L.M.; Ottenwaelder, X.; Stack, T.D.P. Structure and Spectroscopy of Copper–Dioxygen Complexes. *Chem. Rev.* **2004**, *104*, 1013–1046. [[CrossRef](#)] [[PubMed](#)]
75. Lieberman, R.L.; Rosenzweig, A.C. Crystal structure of a membrane-bound metalloenzyme that catalyses the biological oxidation of methane. *Nature* **2005**, *434*, 177–182. [[CrossRef](#)] [[PubMed](#)]
76. Sutradhar, M.; Martins, L.M.D.R.S.; Guedes da Silva, M.F.C.; Mahmudov, K.T.; Liu, C.-M.; Pombeiro, A.J.L. Trinuclear Cu^{II} Structural Isomers: Coordination, Magnetism, Electrochemistry and Catalytic Activity towards the Oxidation of Alkanes. *Eur. J. Inorg. Chem.* **2015**, *23*, 3959–3969. [[CrossRef](#)]
77. Kirillov, A.M.; Shul'pin, G.B. Pyrazinecarboxylic acid and analogs: Highly efficient co-catalysts in the metal-complex-catalyzed oxidation of organic compounds. *Coord. Chem. Rev.* **2013**, *257*, 732–754. [[CrossRef](#)]
78. Bruker. *APEX2 and SAINT*; Bruker, AXS Inc.: Madison, WI, USA, 2004.
79. Sheldrick, G.M. Phase annealing in SHELX-90: Direct methods for larger structures. *Acta Crystallogr. Sect. A: Found. Crystallogr.* **1990**, *A46*, 467–473. [[CrossRef](#)]

80. Sheldrick, G.M. A short history of *SHELX*. *Acta Crystallogr. Sect. A Found. Crystallogr.* **2008**, *A64*, 112–122. [[CrossRef](#)] [[PubMed](#)]
81. Farrugia, L.J. *WinGX* and *ORTEP* for Windows: An update. *J. Appl. Crystallogr.* **2012**, *45*, 849–854. [[CrossRef](#)]



© 2019 by the authors. Licensee MDPI, Basel, Switzerland. This article is an open access article distributed under the terms and conditions of the Creative Commons Attribution (CC BY) license (<http://creativecommons.org/licenses/by/4.0/>).